Isomers of Protonated Octane, $C_8H_{19}^+$

Christa Seitz and Allan L. L. East*

Department of Chemistry and Biochemistry, University of Regina, Regina, Saskatchewan S4S 0A2, Canada

Received: July 24, 2002; In Final Form: September 19, 2002

Ab initio calculations at the MP2/6-31G(d) level of theory have been performed to determine the geometries and relative energies of many isomers of protonated octane (also known as octonium or octanium ions). Five of the 18 structural isomers of octane were considered for protonation, as they provided C−C bonds containing all possible combinations of carbon substitution types (quaternary−tertiary, quaternary−secondary, etc.). All resulting isomers of $C_8H_{19}^+$ feature either a CHC or a CHH 3-center-2-electron (3c2e) bond, although barrierless dissociation into an ion−molecule complex was very common. Octonium ion properties such as relative energies, 3c2e bond geometries, Mulliken partial charges, and the frequency of the most intense infrared absorption, have also been calculated. Each property is correlated to the level of substitution of C atoms in the 3c2e bond. The proton affinities of individual bonds in octane range from 154 to 187 kcal mol^{-1} for C−C bonds and 139 to 150 kcal mol^{-1} for C−H bonds. Alkanium (carbonium) ions of greater than four carbons have never before been studied in this depth.

Introduction

Protonated alkanes ($C_nH_{2n+3}^+$ for acyclic systems) have been observed as fleetingly stable gas-phase ions in mass spectrometers since the 1950s; CH_5^+ was first reported by Tal'roze and Lyubimova[1] in 1952, and $C_2H_7^+$ by Wexler and Jesse[2] in 1962. These ions, also known as carbonium or alkanium ions, generally contain pentacoordinated carbon atoms and unusually extensive fluxional hydrogen-scrambling motions and have low dissociation energies (<20 kcal mol^{-1}).[3,4] They are possible intermediates in reactions of alkanes, in hydrogen or methane-rich conditions in the gas phase, and in superacidic conditions in the condensed phase. Experimental characterization of these ions has been severely limited by the short lifetimes of these ions; most notably, the attempted experimental characterizations[5,6] of $C_2H_7^+$ ran into data interpretation difficulties[7,8] until the publication of two careful analyses in the late 1990s.[3,9] Therefore, theoretical chemistry has been the most useful tool for understanding the behavior of these fleetingly stable ions.

Proponium[10] and butonium[11−13] ions have now been studied in depth via ab initio methods. Selected isomers of protonated alkanes up to the size of octane have been studied as intermediates in carbenium ion chemistry,[14−17] and protonated adamantine has even been studied.[18] The general patterns that have emerged from these works are that (i) the extra proton will produce a 3-center-2-electron (3c2e) bond by joining an existing C−C or C−H bond in the alkane, (ii) a CHC 3c2e isomer will have a lower energy than a CHH 3c2e isomer of equivalent carbon framework,[3,11,13] and (iii) there appear to be trends in CHC isomers with the level of substitution of the C atoms.[13−15,17] There are also some important differences between small alkanes and large alkanes, such as proton affinity[4] and levels of possible carbon substitution. For the mechanisms of Brønsted-acid-catalyzed alkane modification to be properly understood, there is a need to properly analyze the various isomers of a larger protonated alkane and catalog, characterize, and generalize the isomer properties.

There has been no comprehensive study of the isomers of carbonium ions larger than $C_4H_{11}^+$. The current study was designed around octane, because it is the smallest alkane providing all of the possible combinations of substituted carbons for C−C bonds, e.g., secondary−primary (2°C−1°C), quaternary−tertiary (4°C−3°C), quaternary−quaternary (4°C−4°C), and so on. By searching over 200 unique conformations of $C_8H_{19}^+$, and finding 39 minimum-energy structures from them, we can provide here a nice description of carbonium ion properties for use by future researchers in carbocation chemistry.

This project investigated the optimized geometries that resulted from the systematic protonation of five particular structural and conformational isomers of octane. The resulting $C_8H_{19}^+$ isomers include CHC and CHH isomers, as well as many dissociated complexes. We also report relative energies, proton affinities, Mulliken partial charges, and the frequency of the most intense infrared absorption for each of the optimized species.

Theoretical Methods

Molecular electronic energies, optimized (or lowest energy) geometries, Mulliken partial charges, and the infrared spectra for several isomers of octane and octonium ions were calculated using the software suite Gaussian98[19] on an Onyx 2 (SGI) supercomputer at the University of Regina. Molecular geometries and harmonic frequencies were calculated using analytic first and second derivative formulas, as is routine with Gaussian98. All structures presented in this work were confirmed to be minima by the absence of imaginary harmonic frequencies. Reported energies do not include zero-point vibrational energy (ZPVE) corrections; we did test them for roughly 20 isomers, and found relative energies to vary less than ±1.5 kcal mol^{-1}, with very few changes in energy orderings.

Three methods of electronic structure theory were used. The first, B3LYP, is a semiempirical density functional theory (DFT) model.[20,21] The second, MP2, is second-order Møller−Plesset perturbation theory,[22] an ab initio method, for which both the frozen-core-orbital (fc) and the fully correlated (fu) models were applied. The third, CCSD(T), is coupled-cluster theory with single, double, and approximate triple excitations,[23−25] is a

10.1021/jp021724v CCC: $22.00
Published on Web 10/30/2002

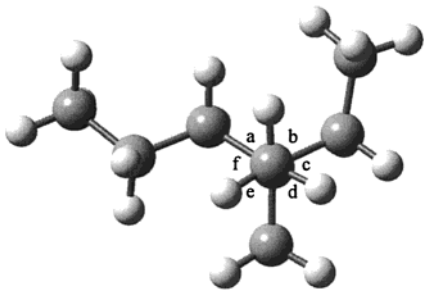

Figure 1. Newman projection along a 1°C−4°C bond of 3,3-dimethylhexane, showing possible dihedral positions for protonating this C−C bond.

highly accurate ab initio method, and was used with the frozen-core-orbital model. Three basis sets were considered for use, namely 6-311G(d), 6-31G(d,p), and 6-31G(d).[19] After preliminary tests, the level of theory chosen for production runs was the MP2(fc) method with the 6-31G(d) basis set.

Generating good initial guesses of carbonium ion geometries was a crucial aspect of the research method. Because large carbonium ions have dissociation energies of less than 10 kcal mol^{-1},[4] a poor initial guess could easily lead to a dissociated system and missing a desired carbonium ion minimum. The optimized internal coordinates for a given structural and conformational isomer of octane was used as an input skeleton, and another line would be added manually to the end, placing the extra H atom in the desired position.

For the CHC carbonium ions the extra proton was initially positioned 0.83 Å from one of the carbons in the desired 3c2e bond, with a CCH bond angle of 24.83°; these values were taken from the optimized CCSD(T) geometry of *trans*-butonium ion (see Calibration section). The dihedral angle for the proton about the C−C bond in the carbonium ion input was chosen to be each of $a = 30°$, $b = 90°$, $c = 150°$, $d = -150°$, $e = -90°$, and $f = -30°$, in the cases where all six positions around the bond are unique (due to the absence of symmetry). Figure 1 demonstrates this using a Newman projection. The bridging proton was chosen to be staggered to the other paraffinic bonds because this is preferred for CHC isomers of smaller protonated alkanes.[3,13] For the CHH carbonium ions the proton was initially placed 0.83 Å from the hydrogen at the C−H bond to be protonated, and the initial H−H−C angle was 70°, with the parameters chosen from previous results for optimized CHH butonium ions.[13] The dihedral angles chosen for H^+ about the C−H bond were $a = 60°$, $b = 180°$, and c = -60° as each C−H bond in octane has three unique staggered positions for the extra proton. In some cases, the dihedral angles were altered slightly to ensure an evenly staggered proton dihedral position with respect to the other atoms.

Initial Considerations

Calibration. To choose an appropriate level of theory, and to gauge its accuracy, several levels of theory were used to optimize the *trans*-butonium ion in which the extra proton resides in the C_2-C_3 bond. The results demonstrate the known fact[4] that the C−H−C angle at the 3c2e bond is very sensitive to level of theory, with values ranging from 122° (MP2(fc)/6-311G(d)) to 156° (B3LYP/6-31G(d,p)), and hence this was chosen as the property for calibration. The CCSD(T)/6-31G-(d,p) value of 132.4° is expected to be the most accurate, but this optimization with GAUSSIAN98 required finite second derivatives and took 1 month to complete; an octonium ion run would take much longer. Hence, we used it to calibrate the faster methods, and of the other levels of theory, the combination of MP2(fc)/6-31G(d) produced a similar value (131.1°). The MP2-(fc)/6-31G(d) level of theory optimized our first $C_8H_{19}^+$ isomer in 3 days, and hence it was chosen for all production runs.

TABLE 1: Relative Energies of Optimized Isomers of Octane

Alkane Form	Relative Energy (kcal mol^{-1})	Figures of Lowest Energy Conformers
2,2,3,3-tetramethylbutane	**0.00**	
3,3-dimethylhexane-1	0.28	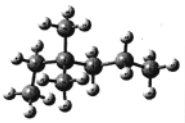
3,3-dimethylhexane-2	**0.09**	
3,3-dimethylhexane-3	0.14	
3,3-dimethylhexane-4	3.16	
3,3-dimethylhexane-5	2.59	
3,3-dimethylhexane-6	2.95	
3,3-dimethylhexane-7	2.54	
3,3-dimethylhexane-8	2.10	
2,2,3-trimethylpentane-1	**0.29**	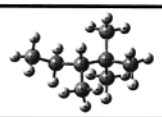
2,2,3-trimethylpentane-2	3.16	
2,2,3-trimethylpentane-3	2.46	
3-ethyl-3-methylpentane-1	**1.02**	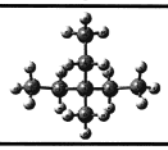
3-ethyl-3-methylpentane-2	1.48	
3-ethyl-3-methylpentane-3	10.80	
3-ethyl-3-methylpentane-4	3.99	
3-ethyl-3-methylpentane-5	3.98	
3-ethyl-3-methylpentane-6	2.08	
2,3-dimethylhexane-1	1.85	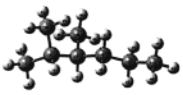
2,3-dimethylhexane-2	2.11	
2,3-dimethylhexane-3	1.25	
2,3-dimethylhexane-4	1.80	
2,3-dimethylhexane-5	**1.24**	
2,3-dimethylhexane-6	1.69	

Choice of Alkane Conformers. Of the 18 structural isomers of octane, five (2,2,3,3-tetramethylbutane, 2,2,3-trimethylpentane, 2,3-dimethylhexane, 3-ethyl-3-methylpentane, and 3,3-dimethylhexane) were sufficient to cover all possible cases of C−C bond substitution (see Introduction). One representative low-energy conformer for each of the five chosen structural isomers of octane was desired, to act as the skeleton for generating low-energy protonated octanes. After we considered major steric interactions, several conformations that were thought to be of low energy were optimized, except for 2,2,3,3-tetramethylbutane, which has only one conformation, and 2,2,3-trimethylpentane, which has only three conformations. The first included in the attempts at finding the lowest energy form of the other three octane isomers was the longest all-trans form. All others were variations from the all-trans differing only by rotations about C−C bonds.

Table 1 gives the resulting energies of the optimized conformers, and the images of the lowest energy conformers of the 5 isomers (whose relative energies are shown in bold type). In two cases, namely 2,3-dimethylhexane-5 and 3,3-dimethylhexane-2, the lowest energy forms were somewhat unexpected. Note the narrow energy range for 23 of the 24 structural and conformational isomers of octane (4 kcal mol^{-1}) and for the 5 chosen conformers (1.24 kcal mol^{-1}). Table 2 compares the relative energies of these 5 conformers with those from experimentally derived heats of formation[26] for the 5 structural isomers, although these would correspond to thermally averaged results for each structural isomer. The ordering of the isomers from lowest energy (2,2,3,3-tetramethylbutane) to highest energy (2,3-dimethylhexane) agrees with the experimental ordering, bolstering confidence in the method.

Nomenclature. A naming system was needed to identify the isomers of $C_8H_{19}^+$. We followed the principle of keeping the

TABLE 2: Octane Conformational Skeletons Used for Protonation

octane isomer	E(rel)[a] MP2 6-31G(d)	E(rel)[a] with ZPVE	E(rel)[a] from exp values of $\Delta H°_{f,298}$	no. of unique C−C bonds	no. of possible proton positions
2,2,3,3-tetramethylbutane	0	0	0	2	4
3,3-dimethylhexane-2	0.09	0.60	1.38	7	42
2,2,3-trimethylpentane-1	0.29	0.71	1.38	7	42
3-ethyl-3-methylpentane-1	1.02	1.74	2.61	5	21
2,3-dimethylhexane-5	1.24	1.85	2.86	7	42

[a] Relative energies in kcal mol^{-1}.

TABLE 3: CHC Octonium Ions, 3c2e Bond Parameters and Other Data (MP2/6-31G(d))

nomenclature	shorthand	C−C substitution	relative energy (kcal/mol)	proton affinity (kcal/mol)	C−H−C angle (deg)	C−C bond length (Å)	most intense IR peak (cm^{-1})
μ23−2,2,3,3-tetramethylbutanium	CHC-1	4°C−4°C	0.00	187.29	180.0	2.525	2248.6
μ23−2,2,3-trimethylpentanium-1	CHC-2	4°C−3°C	7.10	180.48	172.3	2.513	2328.8
μ23−2,2,3-trimethylpentanium-2	CHC-3	4°C−3°C	7.12	180.46	172.8	2.513	2329.3
μ23−2,3-dimethylhexanium	CHC-4	3°C−3°C	14.79	173.74	162.5	2.470	2374.1
μ34−2,2,3-trimethylpentanium-1	CHC-5	3°C−2°C	16.77	170.81	143.0	2.421	2348.2
μ34−2,2,3-trimethylpentanium-2	CHC-6	3°C−2°C	16.83	170.75	150.7	2.469	2372.8
μ34−2,2,3-trimethylpentanium-3	CHC-7	3°C−2°C	16.93	170.65	153.5	2.492	2348.3
μ34−2,3-dimethylhexanium-1	CHC-8	3°C−2°C	19.20	169.33	141.1	2.375	2350.4
μ34−2,3-dimethylhexanium-2	CHC-9	3°C−2°C	19.63	168.89	146.0	2.415	2360.7
μ45−3,3-dimethylhexanium-1	CHC-10	2°C−2°C	24.42	162.95	130.5	2.257	2285.9
μ45−3,3-dimethylhexanium-2	CHC-11	2°C−2°C	24.43	162.94	130.2	2.255	2278.4
μ45−3,3-dimethylhexanium-3	CHC-12	2°C−2°C	24.82	162.55	130.9	2.262	2327.6
μ45−3,3-dimethylhexanium-4	CHC-13	2°C−2°C	24.86	162.51	131.4	2.266	2331.3
μ45−2,3-dimethylhexanium-1	CHC-14	2°C−2°C	27.17	161.36	131.7	2.270	2288.9
μ45−2,3-dimethylhexanium-2	CHC-15	2°C−2°C	27.52	161.01	132.8	2.276	2330.6
μ12−3,3-dimethylhexanium-1	CHC-16	2°C−1°C	29.83	157.54	125.9	2.239	2413.3
μ12−3,3-dimethylhexanium-2	CHC-17	2°C−1°C	29.88	157.50	126.9	2.250	2414.0
μ45−3-ethyl-3-methylpentanium	CHC-18	2°C−1°C	30.69	157.62	127.1	2.261	2431.6
μ12−3-ethyl-3-methylpentanium-1	CHC-19	2°C−1°C	30.90	157.40	127.9	2.270	2423.2
μ12−3-ethyl-3-methylpentanium-2	CHC-20	2°C−1°C	30.93	157.38	129.3	2.287	2432.7
μ45−2,2,3-trimethylpentanium-1	CHC-21	2°C−1°C	31.16	156.42	127.8	2.259	2421.0
μ45−2,2,3-trimethylpentanium-2	CHC-22	2°C−1°C	31.25	156.33	127.7	2.259	2421.9
μ45−2,2,3-trimethylpentanium-3	CHC-23	2°C−1°C	31.30	156.28	129.9	2.284	2412.7
μ56−3,3-dimethylhexanium-1	CHC-24	2°C−1°C	33.37	154.00	128.7	2.270	2418.1
μ56−3,3-dimethylhexanium-2	CHC-25	2°C−1°C	33.38	154.00	128.5	2.268	2417.9
μ56−3,3-dimethylhexanium-3	CHC-26	2°C−1°C	33.38	153.99	128.7	2.270	2416.7

name of the structural isomer of the octane, adding the IUPAC suffix -anium to denote the protonated octane, and adding as a prefix the bridging symbol μ with the number labels of the two carbons bridged by the extra proton (or a number and H if a CH bond is being bridged). Beyond this, if there are multiple rotational conformers of the same structural isomer, we simply denote these by adding a -1, -2, etc. to the parent name. For input file purposes, we also used the letters *a* through *f* to denote the initial dihedral position of the bridging H^+, but we removed this label for the tabulations because of the relative lack of such conformers after optimization. Hence, μ56-3,3-dimethylhexanium-2 refers to 3,3-dimethylhexane with an extra proton bridging the fifth and sixth carbon atoms along the hexane chain and is the second unique minimum of this type that we found. We also use here a shorthand notation (CHC-1, CHH-12, D-9, etc.) for brevity, by which we simply number the CHC-octonium, CHH-octonium, and dissociated complex ions (respectively) in order of increasing energy. We also wish to state in this section that we use the term α or α-carbons to mean the carbon atoms of the 3c2e bond, and β or β-carbons to be the next-nearest carbons to these.

Results and Discussion

CHC Octonium Ion Optimizations. The 5 chosen octane isomer skeletons were inspected for symmetry to determine the number of unique carbon−carbon bonds within the molecule. For each of these unique bonds the number of unique possible proton positions around the bond was determined. Table 2 lists these data for each of the isomers and reveals 151 hypothetical unique minima for this set of 5 skeleton structures. We performed all 151 optimizations. Only 26 unique CHC octonium ions were observed, with 25 runs resulting in duplicates of these, and 100 runs resulting in dissociated complexes (not all were unique).

For the 26 successful runs, the longhand name, shorthand label, and the substitution of the α-carbons are found in Table 3, and the corresponding images can be found in Figure 2. Our strategy of trying multiple choices for the dihedral angle of the extra proton turned out to be very important, for in several cases an isomer remained stable for some choices and dissociated for others. Also, no stable isomers were observed in cases where the α-carbon substitution was severely imbalanced (the 1°C−3°C, 1°C−4°C, and 2°C−4°C cases, in which the bond cleaved and the extra proton left with the least substituted carbon atom).

Relative Energies of the CHC Octonium Ions. The energies of the optimized CHC octonium ions, expressed relative to that of the lowest energy isomer, are tabulated in Table 3 and graphically displayed in Figure 3. The relative energies of these isomers are clearly correlated with the level of substitution of the α-carbons (the carbons of the 3c2e bond). The first point of Figure 3, for the isomer CHC-1 in Table 3, represents a 4°C−4°C bond being protonated, whereas the next two are 4°C−3°C protonated, the next point is 3°C−3°C protonated, the next five points are 3°C−2°C protonated, the next six points are 2°C−2°C protonated, and the last eleven points are 2°C−1°C protonated. This trend is such that the more highly substituted the α-carbons are, the lower the energy will be. This is due to the relatively higher electron density found near highly substituted carbons, resulting in the most stable carbonium ion arrangement. This finding suggests that in the initiation step of

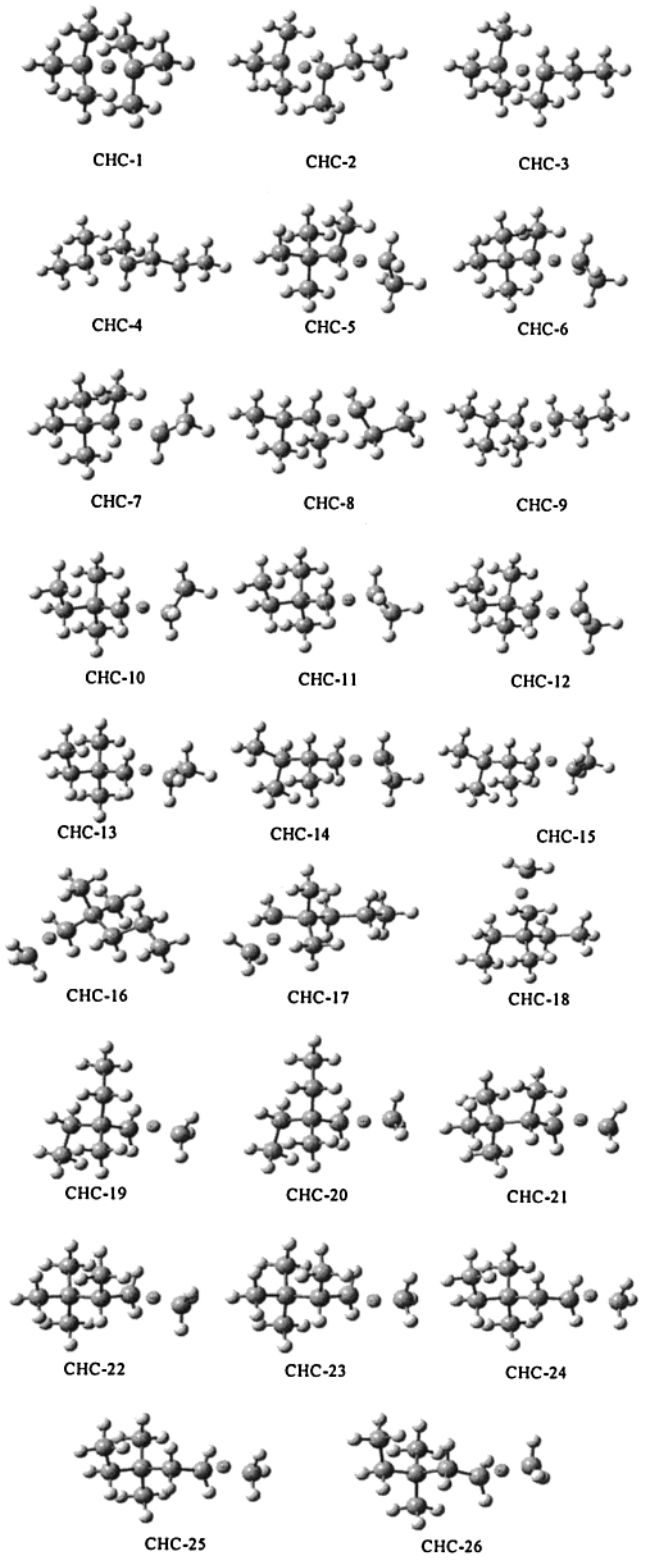

Figure 2. Images of the optimized CHC octonium ions.

the Brønsted-acid-catalyzed cracking mechanism, the Brønsted proton is most attracted to the bond of highest substituted carbons.

Secondary effects can also be seen in the relative energies of Figure 3, due to the level of β-carbon substitution. In the last eleven points (involving 2°C−1°C), the lowest five points occur for cases where the 2° α-carbon is directly bonded to a 4° β-carbon, followed by three cases where the β-carbon is 3°, and then three cases where the β-carbon is 2°. Quaternary β carbons are also responsible for slightly lowering the energies of three 3°C−2°C isomers (CHC-5 through CHC-7) and four 2°C−2°C isomers (CHC-10 through CHC-13). These effects can be explained by the ability of each alkyl substituent to donate electron density to the site of protonation where a positive charge is required to be stabilized.

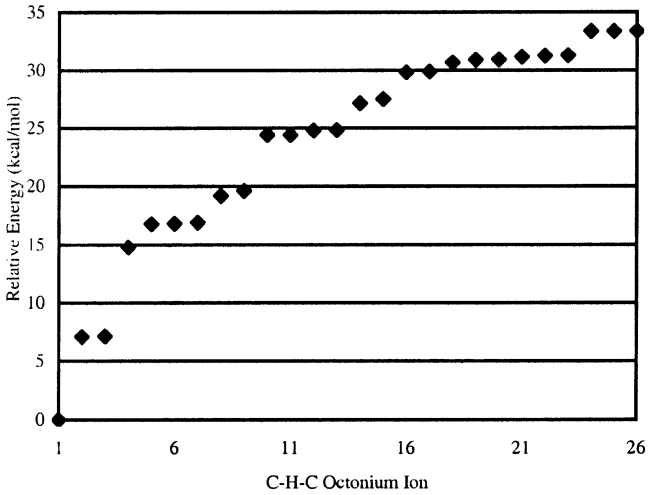

Figure 3. Relative energies of the CHC octonium ions. The α-carbon substitutions are 4°C−4°C (point 1), 4°C−3°C (points 2−3), 3°C−3°C (point 4), 3°C−2°C (points 5−9), 2°C−2°C (points 10−15), and 2°C−1°C (points 16−26).

Very small effects can also be seen, particularly in points CHC-16 though CHC-20, where the substituents bonded to the β 4°C play a role in decreasing the relative energies; however, in this case the benefit is due to extra stability in the parent alkane, and not specifically for the extra proton in this case. Though conformer change is also present here (CHC-18 though CHC-20 show a skeletal trans→gauche change), this effect is minimal.

It is also useful to note from Figure 3 that the relative energies of the CHC octonium ion isomers span a 35 kcal mol^{-1} range, almost 10 times greater than the range spanned by the parent octane isomers. This indicates that carbon atom substitution is an order of magnitude more important for the relative energies of protonated alkanes than of the alkanes themselves.

Boronat, Viruela, and Corma[17] used B3PW91/6-31G(d) geometry optimizations in an investigation of reactions involving carbonium ion intermediates and obtained minima for 6 CHC-octonium ion isomers. They concluded that an increase of C substitution by one will lower the relative energy of the isomer by 6 kcal mol^{-1}. They also noticed an expansion of the C−H−C angle with increasing C substitution. However, their paper was more concerned with reaction energies and activation barriers. Our Table 3 shows that their 6 kcal mol^{-1} rule-of-thumb is approximate, but useful.

Proton Affinities of the C−C Bonds of Octane. These energies were used in conjunction with the five energies of the optimized octane isomers to determine the proton affinities of specific bonds within specific molecular conformers. The calculated proton affinities appear in Table 3. We conclude that a 4°C−4°C center has the greatest proton affinity in alkanes, due to its maximal amount of electron density with which to attract the positive charge of the proton, and that the surprisingly large range of C−C single-bond proton affinities (154−187 kcal mol^{-1}) is experimentally significant.

3c2e Bond Geometries of the CHC Octonium Ions. The C−H−C bond angles and C−C bond lengths involved in the 3c2e bond of the 26 CHC octonium ions are also reported in

Table 3. The most striking feature is the 0.7−1.0 Å increase in C−C bond length upon protonation, which is concomitant with the dramatic weakening of the bond. Again, a general trend with substitution of the α-carbons is clearly seen, although there are some substantial secondary effects. The highest value of the C−H−C angle found (180°) was for the protonated 4°C−4°C bond, the lowest value found (126°) was for a protonated 2°C−1°C bond, and the angle varies somewhat proportionately with the degree of substitution of the carbons involved in the protonated bond. Similarly, the largest C−C bond length found (2.525 Å) was for the protonated 4°C−4°C bond, the smallest value found (2.230 Å) was for a protonated 2°C−1°C bond, and the protonated C−C bond length varies proportionately with the substitution of the carbons at the site of protonation, except for the 2°C−2°C bond lengths, which seem indistinguishable from the 2°C−1°C bond lengths. Both of these trends are due to the fact that more highly substituted carbons have more proton affinity, hence drawing the proton further into the bond, and causing an increase in both the C−H−C angle and the C−C bond length.

The explanation of the secondary effects lies within the nature of the substitution and what happens to the skeleton of the alkane when undergoing optimization. For the carbonium ions CHC-5 and CHC-8, whose C−H−C angles seem too low, it was found that the skeletal backbone undergoes an unanticipated change in structure, leaving a gauche structure rather than the initial all-trans structure. This meant that in the new gauche structures the proton was pulled further away from the C−C bond (due to an extra concentration of electron density on one side of the C−C bond), resulting in a decreased C−H−C angle and C−C bond length. Gauche conversions also occurred for CHC-10, CHC-11, and CHC-14, but the effect here is minimal.

For the protonation sites with 2°C−1°C substitution, the 11 unique structures can be divided into a set of 5 (CHC-16, 17, 18, 21, and 22), in which the bridging proton was staggered with neighboring atoms and bonds, and a set of 6 (CHC-19, 20, 23, 24, 25, and 26), in which the bridging proton was in an *eclipsed* position with a neighboring atom and bond. The increased steric repulsions for a proton in an eclipsed position, rather than a staggered position, caused the 3c2e bond to have an increased C−C bond distance (>2.265 Å) and a resulting increased C−H−C bond angle (>127.8°).

Frash, Solkan, and Kazansky[15] used MP2/6-31G(d) geometry optimizations of hydride-transfer reactions involving carbonium ion intermediates and obtained minima for 1°C−1°C, 2°C−2°C, 3°C−3°C, and 4°C−4°C C−C bonds in ethane, butane, hexane, and octane, respectively. The C−H−C angles were 106°, 134°, 165°, and 180°, respectively. Our results for the last three, with the same level of theory, are 130−133°, 162°, and 180°, with the differences being due to our use of protonated octane exclusively.

Highest Intensity IR Frequencies of the CHC Octonium Ions. Examination of the computed infrared spectrum for each carbonium ion showed that in each case the highest intensity IR absorption was due to the "proton-transfer" vibrational mode. This is the mode in which the bridging proton oscillates from one carbon to the other, with the cationic charge localization correspondingly oscillating in the opposite phase. The animation of these modes shows H^+ motion parallel to the C−C bond, except in cases where the protonation site involves one α-carbon of low substitution; in these cases, the proton displacement vector is tilted for motion between the lower substituted α-carbon and the highest substituted *β*-carbon at the other side of the bond.

The frequency corresponding to this vibrational mode was found to lie between 2240 and 2440 cm^{-1}, for each octonium ion, and have a relative intensity that was on average 12.5 times greater than the next most intense peak. This finding supports an earlier claim[4] that carbonium ions in gas-phase IR experiments may be easily detected by an extremely large absorption in this wavenumber range, providing the species are created and exist long enough to be detected. The frequency (cm^{-1}) for each of the 26 CHC octonium ions is also reported in Table 3.

Once again, there is a trend with the α-carbon substitution, but the frequency does not monotonically increase with decreasing substitution. The 3°C−2°C and 2°C−2°C cases produce surprisingly lower frequencies than anticipated. Our current explanation for this has to do with the room the proton has to oscillate. As the substitution is decreased from 4°C−4°C to 3°C−3°C, the carbon atoms approach each other, giving the proton less room between them, and hence raising the frequency. From 3°C−3°C to 2°C−2°C, the proton is pushed sufficiently far from the C−C bond that it gains increased room by oscillating beside the bond, hence lowering the frequency. From 2°C−2°C to 2°C−1°C, the frequency rises because the displacement vector becomes tilted, with the displacement reduced due to oscillation between an α-carbon and a *β*-carbon. The largest secondary effects are seen in points CHC-10, CHC-11, and CHC-14 of the 2°C−2°C set, which are lower due to the conversion of the carbon skeleton to the gauche form. The data do suggest, however, that an infrared spectrum might be useful not only in identifying the presence of a carbonium ion but also in indicating the substitution at the α-carbons.

Mulliken Partial Charges in the CHC Octonium Ions. The Mulliken partial charges for the CHC isomers of $C_8H_{19}^+$ were also examined. Due to the variety of methods for partial charge computation, the appropriateness of an individual Mulliken partial charge is not as meaningful as relative values or trends in the values, and hence we will focus on the trends.

The partial charges on the C atoms depended almost wholly on the level of carbon substitution, with charges on 4°C, 3°C, 2°C, and 1°C atoms being roughly 0.00, −0.18, −0.35, and −0.51 au, with deviations up to 0.10 au. Interestingly, when the carbon is pentacoordinate (i.e., when it is in the 3c2e CHC bond), these values do not change, except for a 1°C whose charge is −0.60 au if a bridging proton is attached. The alkyl H atoms have charges of +0.15 to +0.25 au, with the lesser values generally appearing for the H atoms far away from the 3c2e bond. However, if the alkyl H is bonded to a 1°C or 2°C carbon in the 3c2e bond, the charge rises to +0.27 to +0.30 au. The partial charge on the bridging proton is actually smaller than on the alkyl hydrogens. These data lend support to statements made by Wiberg et al.,[27] who suggested that molecular ions tend to distribute their charge among the extremity of the system, and H atoms in particular.

The bridging H atom has a large range of possible partial charge values, from +0.01 to +0.24 au, and these are plotted in Figure 4 for our 26 CHC cases, grouped according to α-carbon substitution. The partial positive charge on the proton is observably higher for the low-substitution cases. This is similar to the increase in charge of alkyl H atoms when bonded to such low-substituted α-carbons. We suspect that highly substituted α-carbons, with their increased electron density, are more able to disperse the charge and thereby reduce the partial positive charge on their bonded H atoms (whether alkyl or bridging). An anomaly exists for the 3°C−3°C case, where the partial charge on the H atom is particularly reduced. We

TABLE 4: CHH Octonium Ions, 3c2e Bond Parameters and Other Data (MP2/6-31G(d))

nomenclature	shorthand	substitution of α carbon	substitution of β carbon(s)	relative energy (kcal/mol)	proton affinity (kcal/mol)	H−H bond length (Å)
μ4H-3,3-dimethylhexanium-1	CHH-1	2°	4°, 2°	37.71	149.67	0.907
μ4H-3,3-dimethylhexanium-2	CHH-2	2°	4°, 2°	38.13	149.24	0.860
μ4H-3,3-dimethyhexanium-3	CHH-3	2°	4°, 2°	38.52	148.86	0.869
μ4H-2,3-dimethylhexanium-1	CHH-4	2°	3°, 2°	39.85	148.68	0.896
μ2H-3,3-dimethylhexanium-1	CHH-5	2°	4°, 1°	39.94	147.43	0.885
μ2H-3,3-dimethylhexanium-2	CHH-6	2°	4°, 1°	40.13	147.24	0.881
μ2H-3,3-dimethylhexanium-3	CHH-7	2°	4°, 1°	40.16	147.21	0.881
μ4H-2,3-dimethylhexanium-2	CHH-8	2°	3°, 2°	40.32	148.20	0.869
μ4H-2,2,3-trimethylpentanium-1	CHH-9	2°	3°, 1°	40.46	147.11	0.864
μ5H-3,3-dimethylhexanium-1	CHH-10	2°	2°, 1°	40.75	146.63	0.902
μ5H-3,3-dimethylhexanium-2	CHH-11	2°	2°, 1°	40.83	146.55	0.903
μ4H-2,2,3-trimethylpentanium-2	CHH-12	2°	3°, 1°	41.19	146.39	0.870
μ5H-2,2,3-trimethylpentanium	CHH-13	1°	2°	48.20	139.38	0.897

speculate that the anomaly is in fact with our 4°C−4°C and 4°C−3°C cases and that, if all β-carbons were 2° instead of 1° for these cases, the positive charge on the H atom might be further reduced.

Figure 5 considers the total partial charge of the 3c2e bond, by summing the three Mulliken atomic partial charges of each CHC 3c2e bond. The data in Figure 5 show a very tight, linear

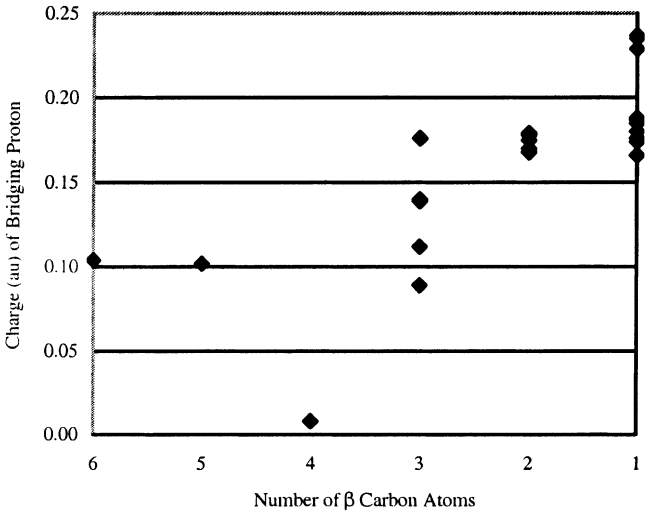

Figure 4. Mulliken partial charges of the bridging H atom of the CHC octonium ions, with the 26 cases sorted by level of substitution of the α carbon atoms.

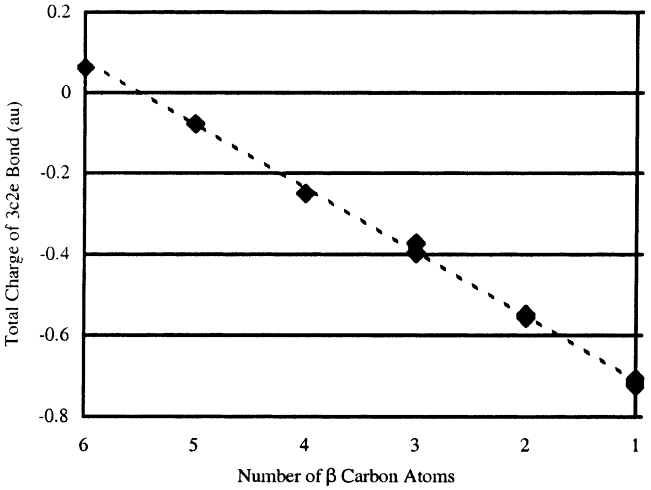

Figure 5. Summed Mulliken partial charges for the 3c2e bond in the CHC octonium ions, with the 26 cases sorted by the level of substitution of the α carbon atoms. Note the considerable overlap of points, compared to Figure 4.

decrease in partial charge of this triatomic region with reduction of C-atom substitution. The scatter is far less than in Figure 4, for reasons that are unclear.

Kazansky, Frash, and van Santen[14] computed partial charges (using CHELPG rather than Mulliken charges) for the bridging proton in 3c2e carbonium cases involving 1°C−1°C, 2°C−2°C, 3°C−3°C, and 4°C−4°C C−C bonds in ethane, butane, hexane, and octane, respectively. They also observed a drop in the charge of the bridging proton with increased C substitution, over the range +0.10 to −0.15, with the charges becoming negative for the 3°C−3°C and 4°C−4°C cases with their charge definition. The drop is steadier than ours, however, without the 3°C−3°C anomaly we observed, possibly because their β-carbon atoms were all 1°C.

CHH Octonium Ion Optimizations. Given the results for the optimized CHC octonium ions, we chose to investigate a smaller subset of the total number of hypothetical CHH octonium ions arising from our 5 alkane skeleton structures. This subset was chosen to cover only the variations in α- and β-carbon substitution afforded by our 5 chosen alkane structures (10 out of a possible 18 variations). For protonation of 1°C−H bonds, those with β-carbons having substitution types 2°, 3°, and 4° were examined. For 2°C−H protonation, the carbon involved in protonation has two β carbons bonded to it, and five particular substitution combinations for the β carbons were considered: 1°C and 2°C, 1°C and 3°C, 1°C and 4°C, 2°C and 3°C, and 2°C and 4°C. For the 3°C−H bond types three different substitution combinations were considered for the β-carbons: 1°C, 1°C, and 3°C, 1°C, 2C, and 3°C, and 1°C, 2C, and 4°C. Only 3 of the 5 structures were actually needed to cover all of these cases, so the study was restricted to protonation of 2,2,3-trimethylpentane, 2,3-dimethylhexane, and 3,3-dimethylhexane. We further restricted ourselves to examining all C−H protonation possibilities for only one of each substitution case listed above; for instance, we examined the two C−H bonds for only one case of a 2° α-carbon bonded to a 3°C and a 2°C. This subset produced 66 hypothetical unique minima, and we performed all 66 optimizations. Only 13 unique CHH octonium ions were observed, with 16 runs resulting in duplicates of these, and 37 runs resulting in dissociated complexes (not all were unique).

For the 13 successful runs, the names and the substitution of the α- and β-carbons are found in Table 4, with the corresponding images in Figure 6. The most stable type of CHH 3c2e bond is that involving a 2° carbon, as 12 of the 13 species fell into this substitution category. The protonation of a 3°C−H bond always resulted in dissociation to form H_2 and a tertiary carbenium ion, whereas in all but one case the protonation of a 1°C−H bond resulted in methane and a rearranged $C_7H_{15}^+$ ion

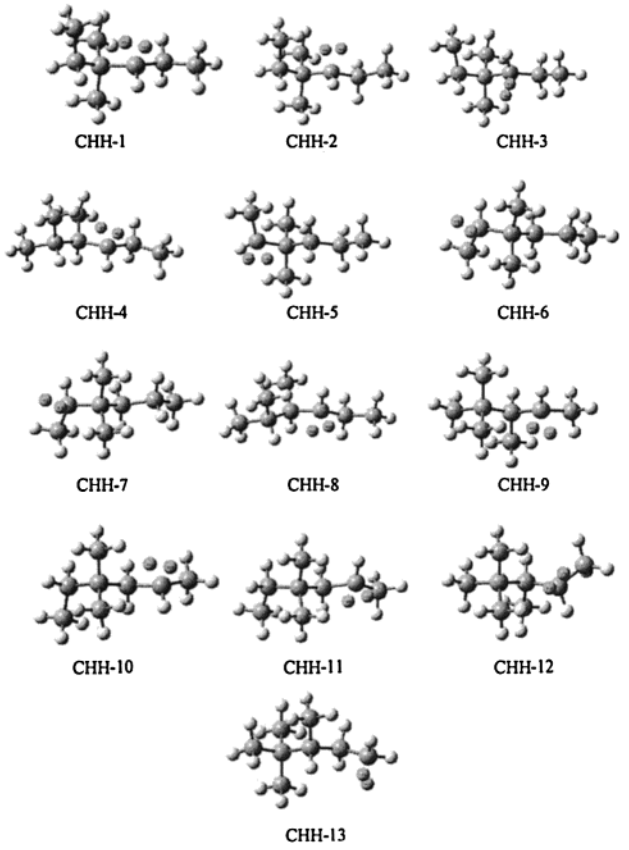

Figure 6. Images of the optimized CHH octonium ions.

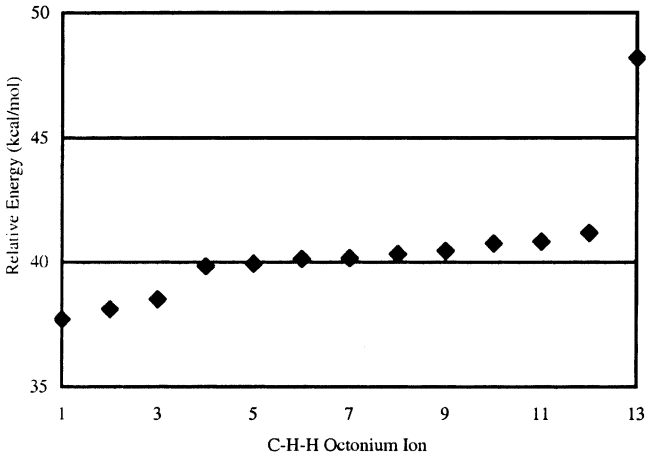

Figure 7. Relative energies of the CHH octonium ions, with respect to the energy of the CHC-1 isomer. The α-carbon substitutions are 2°C (points 1−13) and 1°C (point 14).

(see section entitled Dissociated Complexes for more detail). For the 2° carbons the likelihood of a stable CHH octonium ion is increased if the β-carbons are highly substituted, due to the ability of these β-carbons to better stabilize the charge of the proton.

Relative Energies of the CHH Octonium Ions. The relative energies of the optimized CHH octonium ions, computed relative to the global minimum (CHC-1) for the overall octonium ion potential energy surface, are tabulated in Table 4 and graphically displayed in Figure 7. The most striking feature is the 7 kcal mol^{-1} elevation of CHH-13 relative to the others, due to it being the only case with a 1° α-carbon. Hence, substitution effects are clearly visible in both CHC and CHH isomers. Of the secondary effects present, the most significant one appears to be substitution at the β-carbons, as the three isomers below 39 kcal mol^{-1} correspond to the three cases with the highest degree of β-carbon substitution (4°C and 2°C for the carbon atoms adjacent to the 2° α-carbon).

Esteves, Alberto, Ramirez-Solis, and Mota[11] investigated the isomers of protonated butane using MP4/6-311++G(d,p)//MP2/6-31G(d,p) calculations, and found relative energies of the 1°C−H−H, 2°C−H−H, 2°C−H−1°C, and 2°C−H−2°C isomers to be 16, 12, 5, and 0 kcal mol^{-1}, respectively. Our values for protonated octanes, expressed relative to our lowest 2°C−H-2°C isomer, are 23, 15, 5, and 0. Some of the differences are due to the differently sized molecules, and some are likely due to our lower level of theory; nonetheless, the comparison indicates that our results can be applied to alkanes of all sizes with a certain degree of confidence.

Proton Affinities of the C−H Bonds of Octane. The calculated proton affinities appear in Table 4, where each point represents protonation of an octane to form the listed octonium ion. Note that the proton affinities of C−H bonds (139−150 kcal mol^{-1}) are lower than those of C−C bonds (154−187 kcal mol^{-1}).

Other CHH Octonium Ion Properties. For most of the other CHH octonium ion properties comparable to those studied for the CHC forms (such as: H−H bond length, H−C−H bond angle, and most intense IR frequency), the trends present in the CHC octonium ions were indistinguishable. This is because the range of values was so small that structural differences and steric hindrances play a significant role in the variation. An example of this is given in Table 4 for the H−H distance in the 3c2e bond, showing a variation of only 0.05 Å.

The infrared spectra were also inspected in search of a defining frequency of absorption for these species. There was no dominantly intense peak present in the spectra because a proton-transfer mode does not exist for a CHH 3c2e bond. However, there was a peak in the 2000−2300 cm^{-1} range in each of the spectra that corresponds to a proton-exchange mode where the two H atoms oscillate oppositely toward and away from the C atom. This peak varied in intensity between the spectra, and thus the only way of identifying these species in the infrared might be by the frequency of this peak, as no other absorptions were observed in this region.

The average Mulliken charges on the three atoms (C, H, and H) in the 3c2e bonds of CHH octonium ions are −0.48, +0.30, and +0.30 for the 2°C cases and −0.70, +0.35, and +0.36 for the 1°C case. This demonstrates that the two hydrogen atoms in a CHH 3c2e bond are rather equivalent, and also that the 2°C can dissipate more positive partial charge than the 1°C.

Dissociated Complexes. Many geometry optimizations resulted in dissociated ion−molecule complexes. A total of 53 unique complexes were identified; 46 of these were found during the search for CHC octonium ions, and 7 others were found during the search for CHH octonium ions. We chose to look at the structures and energies of these complexes, because their occurrence in optimization runs indicates that their energies are commensurate or lower than those of carbonium ions, and hence that they represent relevant alternatives that might be present in carbonium ion chemistry. We arranged the 53 complexes into 15 structural groups (A through O), within which the individual ion−molecule complexes have differences only in internal rotation or coordination position. Table 5 contains the dissociated species listed in order of increasing relative energy, the names for each species, and the basic structural type letter label. Images of optimized examples of each structural type are found in Figure 8.

TABLE 5: $C_8H_{19}^+$ Dissociated Complexes

nomenclature	shorthand	structure type	relative energy (kcal/mol)
CH_4•2-methyl-2-butene•ethenium-1	D-1	A	1.53
CH_4•2-methyl-2-butene•ethenium-2	D-2	A	1.54
CH_4•2-methyl-2-butene•ethenium-3	D-3	A	1.55
CH_4•2,3,3,trimethylbut-2-enium-1	D-4	B	1.56
CH_4•2,3,3-trimethylbut-2-enium-2	D-5	B	1.57
CH_4•2-methyl-2-butene•ethenium-4	D-6	A	1.63
CH_4•2-methyl-2-butene•ethenium-5	D-7	A	1.74
CH_4•2,3-dimethylpent-3-enium	D-8	C	2.06
CH_4•3-methylhex-3-enium-1	D-9	D	3.00
CH_4•3-methylhex-3-enium-2	D-10	D	3.11
CH_4•2,3-dimethylpent-2-enium-1	D-11	E	3.15
CH_4•2,3-dimethylpent-2-enium-2	D-12	E	3.19
CH_4•3-methylhex-3-enium-3	D-13	D	3.36
CH_4•3-methylhex-3-enium-4	D-14	D	3.37
CH_4•2,3-dimethylpent-2-enium-3	D-15	E	3.43
CH_4•2,3-dimethylpent-2-enium-4	D-16	E	3.43
CH_4•2,3-dimethylpent-2-enium-5	D-17	E	3.51
CH_4•2,3-dimethylpent-2-enium-6	D-18	E	3.53
CH_4•2,3-dimethylpent-2-enium-7	D-19	E	3.96
CH_4•3-ethylpent-3-enium-1	D-20	F	4.10
CH_4•3-ethylpent-3-enium-2	D-21	F	4.10
CH_4•3-ethylpent-3-enium-3	D-22	F	4.11
CH_4•3-ethylpent-3-enium-4	D-23	F	4.12
CH_4•3-ethylpent-3-enium-5	D-24	F	4.12
CH_4•3-methylhex-3-enium-5	D-25	D	4.49
CH_4•3-methylhex-3-enium-6	D-26	D	4.49
CH_4•3-methylhex-3-enium-7	D-27	D	4.50
CH_4•2-methylhex-2-enium-1	D-28	G	5.15
CH_4•3-methylhex-3-enium-8	D-29	D	5.18
CH_4•3-methylhex-3-enium-9	D-30	D	5.19
CH_4•3-methylhex-3-enium-10	D-31	D	5.20
CH_4•3-methylhex-3-enium-11	D-32	D	5.21
CH_4•3-methylhex-3-enium-12	D-33	D	5.21
C_2H_6•2-methylpent-2-enium-1	D-34	H	6.46
C_2H_6•2-methylpent-2-enium-2	D-35	H	6.52
C_2H_6•2-methylpent-2-enium-3	D-36	H	6.57
C_2H_6•3-methylpent-3-enium-1	D-37	I	6.83
C_2H_6•3-methylpent-3-enium-2	D-38	I	6.95
CH_4•2-methylhex-2-enium-2	D-39	G	6.97
C_2H_6•3-methylpent-3-enium-3	D-40	I	7.41
C_2H_6•3-methylpent-3-enium-4	D-41	I	7.43
C_2H_6•3-methylpent-3-enium-5	D-42	I	7.45
C_3H_8•2-methylbut-2-enium-1	D-43	J	8.75
C_3H_8•2-methylbut-2-enium-2	D-44	J	8.95
CH_4•2-butene•p-propenium	D-45	K	10.68
CH_4•propene•*tert*-butenium-1	D-46	L	14.22
CH_4•propene•*tert*-butenium-2	D-47	L	14.32
H_2•2,3-dimethylhex-3-enium-1	D-48	M	15.54
H_2•2,3-dimethylhex-3-enium-2	D-49	M	15.59
H_2•2,3-dimethylhex-3-enium-3	D-50	M	16.43
H_2•2,3-dimethylhex-2-enium-1	D-51	N	17.32
H_2•2,3-dimethylhex-2-enium-2	D-52	N	18.74
CH_4•ethene•2-methylbut-2-enium	D-53	O	26.60

Most of these complexes involve a small alkane and a carbenium ion with the charge located on a classical tertiary sp^2 carbon atom. However, in structure types A, K, L, and O, the carbenium moiety features a 3-carbon unit that can be considered either a 3c2e bond (with a C−C 2c2e bond in addition, and one pentacoordinated C) or a π-complex of a C═C double bond to a tricoordinate charged C. In Table 5 our nomenclature treats it as a π-complex, but the reader should be aware that the charge is considerably delocalized, the complex is rather tight, and the energies are quite variable.

In structure types A through G and in K, L, and O, the alkane fragment is methane, leaving a $C_7H_{15}^+$ carbenium ion. In structure types H and I, the alkane fragment is ethane, and for type J it is propane. The remaining two structure types, M and N, are those in which protonation attempts were made at a

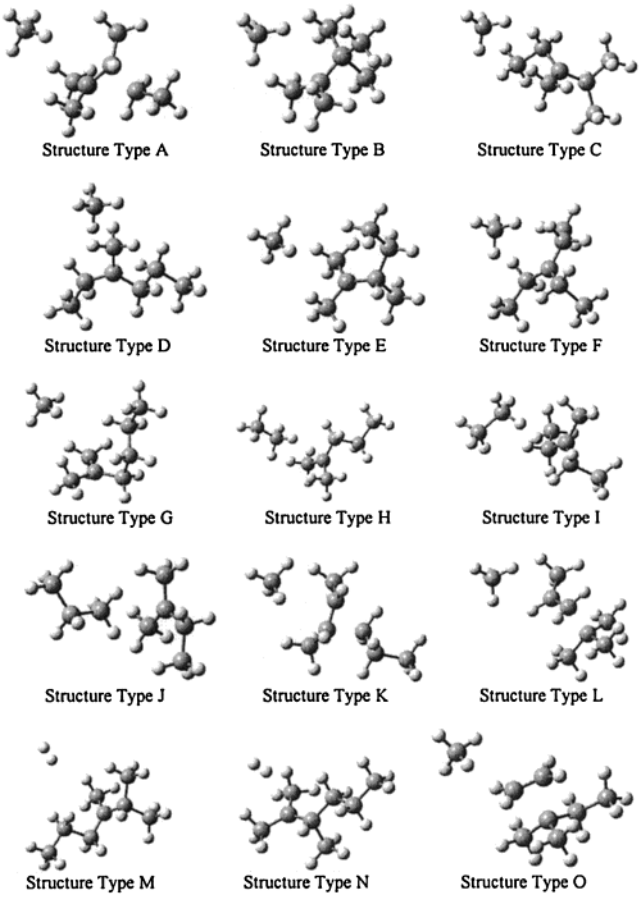

Figure 8. Images of some of the optimized $C_8H_{19}^+$ dissociated complexes, classified by structure type.

3°C−H bond, and which all resulted in the loss of H_2, thus producing complexes between H_2 and a $C_8H_{17}^+$ carbenium ion.

Carbon−carbon bond shifting was evident in several of these optimizations, and occurred in all cases in which the straightforward dissociation of the protonated octane would have resulted in a nontertiary carbocation. In these cases there was one of three different means by which the dissociating octonium ion created the tertiary carbocation: hydride shift (D-8, D-10, D-28, D-39), methanide shift (D-21, D-24, D-25), and ethanide shift (D-14).

Relative Energies of the Dissociated Species. The computed energies of the 53 unique ion−molecule complexes, computed relative to the global minimum (CHC-1) for the $C_8H_{19}^+$ potential energy surface, are listed in Table 5 and graphically displayed in Figure 9.

The trend for the "triple complexes" (structures A, K, L, and O, featuring the tight π-complex or CCC 3c2e bond) is that energy increases with decreasing substitution on the alkene moiety. In structure type A, the alkene unit (2-methyl-2-butene) has 3 substituents bonded to the double-bond carbon atoms, whereas in types K, L, and O, the number of these substituents is 2, 1, and 0, respectively. The energy differences of K, L, and O complexes (relative to A) are roughly 9, 13, and 25, respectively. This trend suggests that for even longer alkanes, there would be another, lower energy complex where the alkene unit has 4 substituents.

The trend for the isomers featuring classical tertiary carbenium ions (B through J, and M and N) is that energy increases with decreasing substitution of the carbons next to the positively charged, sp^2-hybridized, tertiary-substituted carbon. Types B through G are methane•carbenium ion complexes, and the

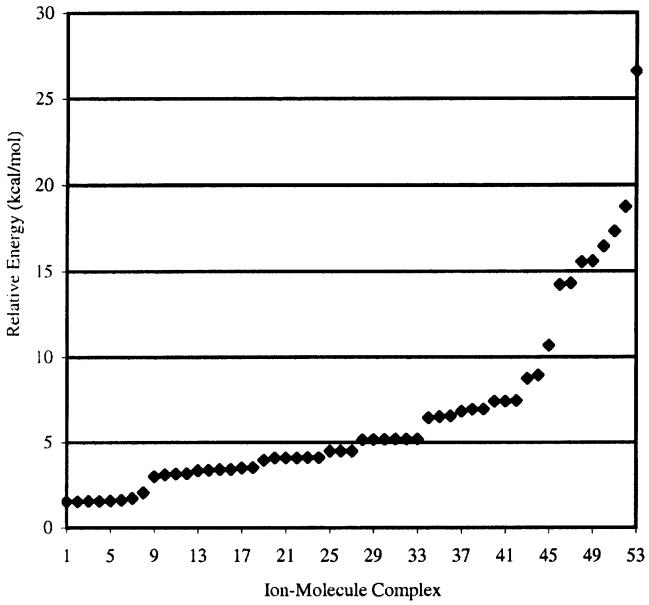

Figure 9. Relative energies of the dissociated complexes, with respect to the energy of the CHC-1 isomer.

neighboring carbon sets in these cases are {4°C, 1°C, 1°C}, {3°C, 2°C, 1°C}, {2°C, 2°C, 1°C}, {3°C, 1°C, 1°C}, {2°C, 2°C, 2°C}, and {2°C, 1°C, 1°C}, respectively, with the energies generally increasing in this order. Structure types H and I are ethane•carbenium ion complexes, and type J is a propane• carbenium ion complex; the raised energies of these complexes relative to methane•carbenium ion complexes indicate the following general trend in these dissociations: the smaller the product alkane is, the more thermally favored the dissociation is. This agrees with a previous finding.[4]

Structure type D is of special interest because we obtained many versions, spanning a 2.2 kcal mol^{-1} energy range that encased the energies found for the structure groups E and F. The variety is due to the internal rotation positions of the ethyl and propyl substituents. The lower energy members of this group (D-9, D-10) have no bonds eclipsing, the next set (D-13, D-14) has one partially eclipsing bond, the next set (D-25 through D-27) has many partially eclipsing bonds, and the highest energy set (D-29 through D-33) has two instances of two C−C bonds completely eclipsing. The higher energy set resulted in minima only because of hyperconjugation. The type D structures demonstrate that steric hindrance is a secondary effect in the energies of these ion−molecule complexes, producing variances of as much as 2.2 kcal mol^{-1}.

Finally, structure types M and N are complexes of H_2 with a $C_8H_{17}^+$ carbenium ion. The charged carbon atom is neighbored in these cases by {3°C, 2°C, 1°C} and {3°C, 1°C, 1°C} for type M and N, respectively. The high energy of these structures suggests that H_2 dissociation would occur only from direct C−H protonation, and not from a scrambling process.

Conclusions

Isomers of $C_8C_{19}^+$ have been studied via ab initio methods using the Gaussian98 software suite. The MP2/6-31G(d) level of theory has been applied as it was found to provide more accurate results than B3LYP for the C−H−C bond angle, when compared to the high-accuracy CCSD(T)/6-31G(d,p) method for protonated butane.

For the CHC octonium ions, 26 of the 151 isomers thought to be possible (from the 5 chosen skeletal structures of octane) were found to exist at the applied level of theory. Trends in the energies, proton affinities, C−C bond lengths, and C−H−C bond angles are strongly related to the level of substitution of the α-carbon atoms (those involved in the 3c2e bonds): as the substitution is increased, the relative energy decreases, the proton affinity of the original bond increases, and the C−C bond length and C−H−C bond angle both increase. A signature infrared frequency for the octonium ions has been found to lie between 2249 and 2421 cm^{-1} and varies inversely with the α-carbon substitutions except for the 2°C−2°C and 3°C−2°C cases, which lie at lower frequencies than expected. Mulliken partial charges indicate that the partial charge on the bridging proton is between 0 and +0.25 au, and drops as the α-carbon substitution increases, due to the increased ability of highly substituted α-carbons to dissipate the charge further down the molecule.

For the CHH octonium ions, only 13 of the 66 predicted isomers were found to exist at the applied level of theory. Twelve of the 13 cases involved a secondary carbon atom in the CHH 3c2e bond, and hence trends within the CHH octonium ion isomers were not as clear. These isomers all lie higher in energy than all CHC isomers.

It was generally found that the protonation of 4°C−2°C, 4°C−1°C, 3°C−1°C, and 3°C−H bonds do not result in stable

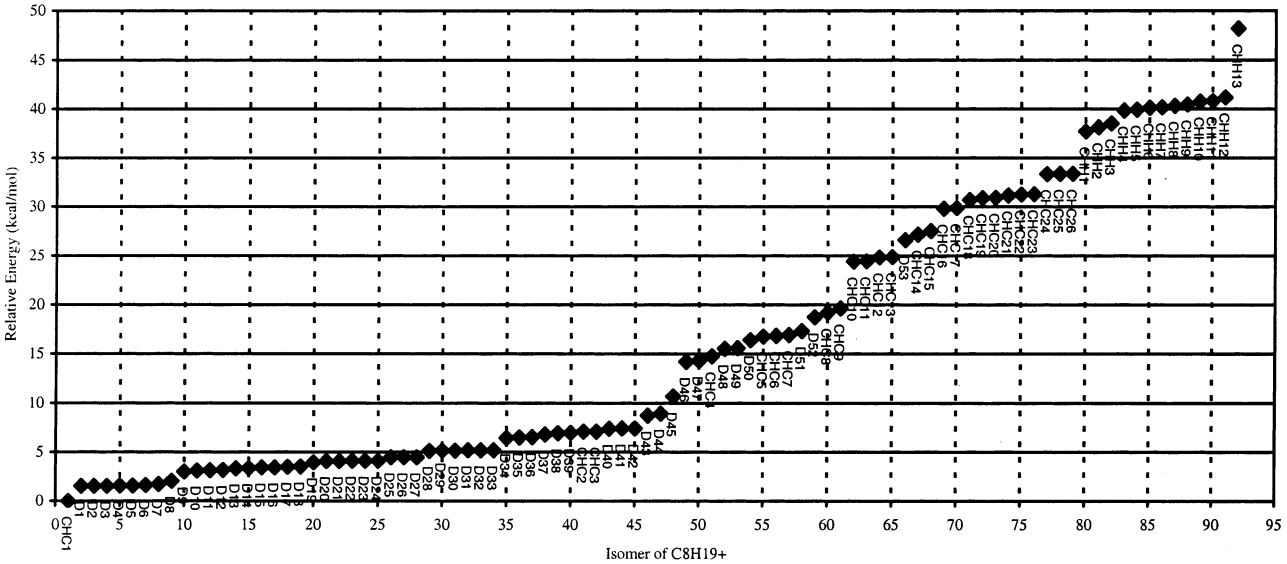

Figure 10. Overall relative energy plot, for all optimized structures of $C_8H_{19}^+$ including dissociated complexes.

octonium ions, with their optimizations instead leading to dissociated ion−molecule complexes. Several other protonation cases led to dissociated complexes, and all 53 unique dissociated complexes were analyzed in terms of structure and energy. The complexes involved a small alkane molecule (usually methane) with a carbenium ion, although the 3°C−H protonations produced an H_2•carbenium ion complex. The carbenium ions in these complexes fell into two classes: a classical structure with a trivalent tertiary-substituted carbon, or a nonclassical structure featuring a CCC 3c2e bond with an additional 2c2e C−C bond, alternatively viewed as a tight π-complex of a C═C double bond with a trivalent cationic carbon atom. Relative energies of the classical-carbenium-ion complexes generally increased with the decreasing level of substitution of the carbon atoms next to the charge-carrying atom, whereas for the nonclassical ones they increased with the decreasing level of substitution of the C═C carbon atoms.

The relative energies from Tables 3−5, for all of the octonium ions and dissociated species found, have been put together to create an overall relative-energy plot, found in Figure 10. The data points in Figure 10 are labeled with the shorthand naming system. The lowest energy form of $C_8H_{19}^+$ is an octonium ion having the central C−C bond in 2,2,3,3-tetramethylbutane protonated. The next lowest set of isomers is that dealing with the dissociated species. This is a significant finding, because it suggests that the octonium ions (particularly branched ones) are very likely to dissociate after having been protonated. A great variety of dissociated products are possible at energies lower than the next preferred carbonium ion, a CHC isomer with a protonated 4°C−3°C bond (~7 kcal mol^{-1} in the figure). Figure 10 also shows that all CHH octonium ions are higher in energy than all the CHC octonium ions, lying in the range 38−42 kcal mol^{-1}, which suggests that in the initial conversion of an alkane to a carbonium ion, if a CHH carbonium ion were initially created, it would rapidly convert to a CHC carbonium ion or a dissociated species.

The results presented here can be generally applied to protonated alkanes of any size.

Acknowledgment. The Institute of Computational Discovery (University of Regina) is thanked for computational resources. NSERC (Canada) is thanked for research funding.

References and Notes

(1) Tal'roze, V. L.; Lyubimova, A. L. *Dokl. Akad. Nauk SSSR* **1952**, *86*, 909; *Chem Abstr.* **1953**, *47*, 2590.

(2) Wexler, S.; Jesse, N. *J. Am. Chem. Soc.* **1962**, *84*, 3425.

(3) East, A. L. L.; Liu, Z. F.; McCague, C.; Cheng, K.; Tse, J. S. *J. Phys. Chem. A* **1998**, *102*, 10903.

(4) Hunter, K. C.; East A. L. L. *J. Phys. Chem. A* **2002**, *106*, 1346.

(5) Hiraoka, K.; Kebarle, P. *J. Am. Chem. Soc.* **1976**, *98*, 6119.

(6) Yeh, L. I.; Price, J. M.; Lee, Y. T. *J. Am. Chem. Soc.* **1989**, *111*, 5597.

(7) Obata, S.; Hirao, K. *Bull. Chem. Soc. Jpn.* **1993**, *66*, 3271.

(8) Carneiro, J. W.d. M.; Schleyer, P. v. R.; Saunders: M.; Remington, R.; Schaefer, H. F., III; Rauk, A.; Sorensen, R. S. *J. Am. Chem. Soc.* **1994**, *116*, 3483.

(9) Fisher, J. J.; Koyanagi, G. K.; McMahon, T. B. *Int. J. Mass Spectrosc.* **2000**, *196*, 491.

(10) Esteves, P. M.; Mota, C. J. A.; Ramírez-Solís, A.; Hernandez-Lamoneda, R. *J. Am. Chem. Soc.* **1998**, *120*, 3213.

(11) Esteves, P. M.; Alberto, G. G. P.; Ramírez-Solís, A.; Mota, C. J. A. *J. Phys. Chem. A* **2000**, *104*, 6233.

(12) Mota, C. J. A.; Esteves, P. M.; Ramírez-Solís, A.; Hernandez-Lamoneda, R. *J. Am. Chem. Soc.* **1997**, *119*, 5193

(13) Seitz, C.; East, A. L. L. University of Regina, unpublished work.

(14) Kazansky, V. B.; Frash, M. V.; van Santen, R. A. *Catal. Lett.* **1997**, *48*, 61.

(15) Frash, M. V.; Solkan, V. N.; Kazansky, V. B. *J. Chem. Soc., Faraday Trans.* **1997**, *93*, 515.

(16) Boronat, M.; Viruela, P.; Corma, A. *J. Phys. Chem B* **1997**, *101*, 10069.

(17) Boronat, M.; Viruela, P.; Corma, A. *J. Phys. Chem B* **1999**, *103*, 7809.

(18) Esteves, P. M.; Alberto, G. G. P.; Ramírez-Solís, A.; Mota, C. J. A. *J. Phys. Chem. A* **2001**, *105*, 4308.

(19) Frisch, M. J.; Trucks, G. W.; Schlegel, H. B.; Scuseria, G. E.; Robb, M. A.; Cheeseman, J. R.; Zakrzewski, V. G.; Montgomery, J. A.; Stratmann, R. E.; Burant, J. C.; Dapprich, S.; Millam, J. M.; Daniels, A. D.; Kudin, K. N.; Strain, M. C.; Farkas, O.; Tomasi, J.; Barone, V.; Cossi, M.; Cammi, R.; Mennucci, B.; Pomelli, C.; Adamo, C.; Clifford, S.; Ochterski, J.; Petersson, G. A.; Ayala, P. Y.; Cui, Q.; Morokuma, K.; Malick, D. K.; Rabuck, A. D.; Raghavachari, K.; Foresman, J. B.; Cioslowski, J.; Ortiz, J. V.; Stefanov, B. B.; Liu, G.; Liashenko, A.; Piskorz, P.; Komaromi, I.; Gomperts, R.; Martin, R. L.; Fox, D. J.; Keith, T.; Al-Laham, M. A.; Peng, C. Y.; Nanayakkara, A.; Gonzalez, C.; Challacombe, M.; Gill, P. M. W.; Johnson, B. G.; Chen, W.; Wong, M. W.; Andres, J. L.; Head-Gordon, M.; Replogle, E. S.; Pople, J. A. *Gaussian 98*, Revision A.9; Gaussian, Inc.: Pittsburgh, PA, 1998.

(20) Becke, A. D. *J. Chem. Phys.* **1993**, *98*, 5648.

(21) Lee, C.; Yang, W.; Parr, R. G. *Phys. Rev. B* **1988**, *37*, 785.

(22) Møller, C.; Plesset, M. S. *Phys. Rev.* **1934**, *46*, 618.

(23) Cizek, J. *Adv. Chem. Phys.* **1969**, *14*, 35.

(24) Pople, J. A.; Head-Gordon, M.; Raghavachari, K. *J. Chem. Phys.* **1987**, *87*, 5968.

(25) Bartlett, R. J. *J. Phys. Chem.* **1989**, *93*, 1697.

(26) Weast, R. C. *CRC Handbook of Chemistry and Physics*, 67th ed.; CRC Press: Boca Raton, FL, 1986.

(27) Wiberg, K. B.; Schleyer, P.v. R.; Streitwieser, A. *Can. J. Chem.* **1996**, *74*, 892.